Contacted Resistance Measurements for the Quantification of Boron-Hydrogen Pairs in Crystalline Silicon

Clemens Winter and Axel Herguth [a)]

University of Konstanz, Department of Physics, 78457 Konstanz, Germany

[a)]Corresponding author: axel.herguth@uni-konstanz.de

Abstract. The methodology of directly contacted resistance measurements for the quantification of boron-hydrogen (BH) pairs in crystalline silicon (Si) is presented. Temperature is found to be the most critical error source. It is demonstrated that the methodology can be used to quantify changes in BH pair concentration down to the sub-permille level which corresponds to the low 10^{12} cm^{-3} range for 1 Ω·cm Si material commonly used for solar cells. It is furthermore demonstrated that BH dynamics can be observed not only in impurity-lean FZ-Si, but also in impurity- and defect-richer Cz-Si and mc-Si. As the used sample design enables both, lifetime and BH measurements, a correlation study of LeTID and BH dynamics was performed suggesting that BH pairs are probably not the LeTID-related defect species. However, the coincident onset of both dynamics may be interpreted as a common mode of action like the splitting of hydrogen dimers.

INTRODUCTION

For quite a long time it is known that hydrogen is able to passivate otherwise recombination active defects in crystalline silicon and at its surface, hence improving material quality. For that reason, hydrogenation is a vital part of today's solar cell manufacturing. Commonly this is synergistically implemented by depositing a hydrogen-rich anti-reflective and passivating coating like silicon nitride (SiN_x:H) combined with a high temperature firing step used to concurrently release hydrogen and form screen-printed contacts. However, in the recent past it has become clear that hydrogen plays a critical role in Light- and elevated Temperature Induced Degradation (LeTID), e. g. [1] [2], and hydrogenation may deteriorate material quality as well.

Many studies on hydrogen are of qualitative nature only because quantifying hydrogen in crystalline silicon has always proven challenging due to its low concentration (below 10^{15} cm^{-3}) compared to a rather bad detection limit in many elemental analysis techniques. Secondary ion mass spectrometry (SIMS), probably the most commonly applied elemental analysis technique, can reliably detect ^{1}H only in concentrations above 10^{18} cm^{-3} [3]. Exploiting the natural isotope abundance ratio, ^{2}H detection is possible even down to ~10^{14} cm^{-3}, but such studies require a rather expensive deuterium source.

A different approach to the quantification of hydrogen in crystalline silicon goes back a few decades. Hydrogen tends to bind to dopant atoms like boron, negating their doping activity [4] [5] [6]. This allows for an indirect quantification of hydrogen via its impact on charge carrier density [7] [8] [9] [10] and thus electrical resistivity and conductivity [4] [11]. Walter et al. [12] exploited this approach using the eddy current technique used in common photoconductance decay (PCD) setups. However, measuring resistivity accurately with that setup has proven challenging; it is simply not build for that purpose. Hence, we decided to apply resistance measurements on directly contacted, metallized samples promising a better accuracy. This contribution deals with the mathematical framework behind this approach, quantifies its limits and demonstrates its application to different silicon materials. In addition, an exemplary application in the correlation of BH pair concentration with LeTID is shown.

METHODOLOGY

The following description focuses on p-type material, but the method would work in n-type material with a few adaptions as well. A thorough discussion of the method, especially with respect to error sources, can be found in [13]. Atomic hydrogen predominantly exists as H^+ in p-type material [14], hence, the pairing reaction $H^+ + B^- \leftrightarrows BH^0$ would not change the background hole concentration. However, solubility of atomic hydrogen is very low in crystalline silicon and thus this reaction can only be an intermediate step. After a rapid high temperature step hydrogen is assumed to be mainly present in form of neutral dimers H_{2A}, where 'A' refers to a specific configuration [15]. These dimers need to be split up before pairing with boron in the total reaction $H_{2A} + 2\,B^- + 2\,h^+ \leftrightarrows 2\,BH^0$ consuming holes (h^+). Hence, the formation of a BH pair concentration $[BH]$ changes the equilibrium hole concentration p_0

$$p_0 = N_{\mathrm{dop}} - [BH] \tag{1}$$

that then deviates from the otherwise present ionized net dopant concentration N_{dop}. This impacts resistivity ρ

$$\rho^{-1} = q \cdot (\mu_{\mathrm{p}} \cdot p_0 + \mu_n \cdot n_0) \approx q \cdot \mu_{\mathrm{p}} \cdot p_0 \tag{2}$$

which is dominated by hole conduction in the p-type material used here ($n_0 \ll p_0$). Resistivity depends, besides hole concentration p_0, also on hole mobility μ_{p} and elementary charge q. Assuming a cuboid shaped sample with cross-section A and contacts separated by a distance d, resistance R is given by

$$R = \rho \cdot \frac{g \cdot d}{A} \tag{3}$$

introducing a geometry correction factor $g \approx 1$ to compensate for deviations from the ideal cuboid shape. For our geometry, simulation yields g = 1.02. Combining these equations, BH pair concentration [BH] is given by

$$[BH] = N_{\mathrm{dop}} - \frac{g \cdot d}{q \cdot A} \cdot \frac{1}{\mu_{\mathrm{p}} \cdot R} \tag{4}$$

However, N_{dop} typically being of the order of $10^{16}\,\mathrm{cm}^{-3}$ is much larger than the expected BH concentration (see experiments) and even a comparatively small error of ±1 % in N_{dop} would already yield an apparent BH pair concentration of $\pm 10^{14}\,\mathrm{cm}^{-3}$. In addition, there might already be BH pairs present that impact net doping, and it is therefore impossible to say what the true net doping concentration is. Under the assumption of a constant net doping background, taking the difference between two measurements B(efore) and A(fter) a treatment step eliminates this problem and yields the change in BH pair concentration

$$\Delta[BH] = \frac{g \cdot d}{q \cdot A} \cdot \left(\frac{1}{\mu_{\mathrm{p,B}} \cdot R_{\mathrm{B}}} - \frac{1}{\mu_{\mathrm{p,A}} \cdot R_{\mathrm{A}}} \right) \tag{5}$$

It should be noted that even though N_{dop} does not explicitly occur in the above equation any more, it is still of some relevance because hole mobility μ_{p} depends on total hole concentration that changes as BH pairs form. An educated guess of a constant μ_{p} is helpful for a rough first calculation. For higher reliability, hole mobility and hole concentration can be determined self-consistently from a combination of equations 2 and 3

$$\mu_{\mathrm{p}} \cdot p_0 = \frac{g \cdot d}{q \cdot A} \cdot \frac{1}{R} \tag{6}$$

In this paper, hole mobility is taken from [16], including a multitude of background models [17] [18] [19] [20] [21].

SAMPLE AND MEASUREMENT SETUP

In the first experiment, boron-doped FZ-Si wafers (1 Ω·cm, 250 µm thick, 5x5 cm^2) with thin silicon oxide (wet-chemically grown by the manufacturer) are bifacially coated with ~70 nm hydrogen-rich SiN_x:H (T_{dep} ~ 450°C, direct PECVD, centrotherm international AG) that releases hydrogen during a subsequent rapid thermal annealing step in a belt furnace (measured peak temperature 745°C). To allow for directly contacted resistance measurements, aluminium electrodes are deposited via thermal evaporation on the sample in form of two parallel double-stripes that are later on used for highly accurate four-terminal measurements. The spacing between the inner stripes was chosen >40 mm to allow for PCD measurements, i.e., not to interfere with the used eddy current technique in the WCT-120 lifetime tester (Sinton Instruments) [22] [23]. Direct contact to the silicon through the SiN_x:H layer is established by a multitude of laser fired contacts (LFCs) [24].

In the second experiment, FZ-Si (2.8 Ω·cm), Cz-Si (2.1 Ω·cm) and mc-Si (1.2 Ω·cm) are saw-damage etched (final thickness 160 µm), cleaned in a piranha solution (H_2O_2, H_2SO_4), HF-dipped, passivated by ~100 nm SiN_x:H ($T_{dep} \sim 400$°C, direct PECVD, Plasmalab 100, Oxford Instruments) and fired in a belt furnace (variable peak temperature). Metal electrodes are prepared as described above.

In the third experiment, FZ-Si (2.0 Ω·cm) is etched (final thickness 220 µm), cleaned in a piranha solution (H_2O_2, H_2SO_4), HF-dipped, passivated by 5 nm AlO_y (ALD, FlexAl, Oxford Instruments) capped by ~100 nm SiN_x:H (same as in the second experiment) and fired in a belt furnace (measured peak temperature 803°C). Metal electrodes are prepared as described above.

In order to trigger BH pair formation, the samples are annealed in darkness at an elevated temperature of either 180°C or 220°C on a hotplate. For the resistance measurements, the sample is removed from the hotplate and placed on a water-cooled mount at a temperature of 25°C. The resistance measurement is done with a 6½-digit digital multimeter (Keithley 2000) in four-terminal configuration in a light-tight housing. Lifetime is measured with the above mentioned WCT-120 lifetime tester.

EXPERIMENT 1: PROOF-OF-PRINCIPLE

In the first experiment, SiN_x:H passivated boron-doped FZ-Si samples (I+II) are annealed at 180°C in darkness to trigger BH pair formation. A reference sample (III) is stored at ~20°C in darkness. Figure 1(a) shows the development of the measured resistance, Fig. 1(b) the calculated change in BH pair concentration $\Delta[BH]$ with respect to the first measurement point. As can be seen there are slight differences in resistance between the samples that vanish almost completely in $\Delta[BH]$. The changes of sample I and II match almost perfectly a double exponential function

$$\Delta[BH] = -A_1 \cdot \exp\left(-\frac{t}{t_1}\right) + A_2 \cdot \exp\left(-\frac{t}{t_2}\right) - (A_2 - A_1) \quad (7)$$

being the solution for first order kinetics of BH pair formation and dissociation according to the reaction

$$\mathrm{H_{2A}} + 2\,\mathrm{B^-} + 2\,\mathrm{h^+} \rightleftharpoons 2\,\mathrm{BH^0} \rightleftharpoons 2\,\mathrm{HX^0} + 2\,\mathrm{B^-} + 2\,\mathrm{h^+} \quad (8)$$

While the first part of the reaction is well studied, the second part is still under discussion. The increase in hole concentration is likely caused by a reactivation of boron as dopant, requiring hydrogen to stay neutral. However, atomic hydrogen would inevitably charge positively in p-type material [14]. Therefore, hydrogen must either find a binding partner or effuse. It cannot be excluded that the binding partner is hydrogen itself, hence HX could be a dimeric configuration (H_{2C}) that differs from H_{2A} as suggested by Voronkov and Falster [15].

The untreated sample III shows unsystematic scattering (standard deviation 7×10^{12} cm^{-3}) demonstrating the reproducibility of the measurement as BH pair formation is expected to occur very slowly at ~20°C. The almost perfect fit of the double exponential function to samples I and II already suggests that the error in $\Delta[BH]$ is that small.

In order to test the limits of BH pair quantification via direct resistance measurements, a sample was left in the measurement setup for several days while its resistance was permanently monitored. The derived apparent change in BH pair concentration is shown in Fig. 2. Three details stand out: First, there is a slight upward trend that might indicate a slow formation of BH pairs even at 25°C; ~4×10^{12} cm^{-3} in 7 days. Such a trend might be hidden in the scattering of Fig. 1. Second, overall scattering is smaller than observed in Fig. 1. Third, there is a prominent oscillation visible that is most likely not related to cyclic formation of BH pairs. In contrast, the 1 day period rather implies a day-night-cycle influencing the setup. The answer to the last two observations most probably lies in the temperature dependence of the hole mobility μ_p. From equation 5 it follows that a temperature deviation δT between actual temperature and assumed temperature leads to an apparent change in BH pair concentration [13]

$$\delta\Delta[BH] = p_0 \cdot \frac{1}{\mu_p}\frac{d\mu_p}{dT} \cdot (\delta T - \delta T_0) \quad (9)$$

The relative change in mobility amounts to -6.4 ‰/K at 25°C for the used 1 Ω·cm material ($p_0 \sim 1.5\times10^{16}$ cm^{-3}). Thus an unnoticed temperature deviation of ~15 mK is enough to trigger the observed sine wave oscillation. And this dependence likely explains the smaller scattering in Fig. 2 compared to Fig. 1. For each measurement in Fig. 1, the light-tight chamber had to be opened to place the sample on the water-cooled sample mount thus disturbing thermal equilibrium each time. It might take a few minutes for the whole system to equilibrate again, and thus the unnoticed temperature deviations are likely higher. Generally speaking, the lowest BH pair concentration that can be unambiguously detected depends on the doping concentration and on the ability to control temperature. Properly done, changes in BH concentrations in the sub-permille range, i.e. low 10^{12} cm^{-3} range in 1 Ω·cm material, can be quantified.

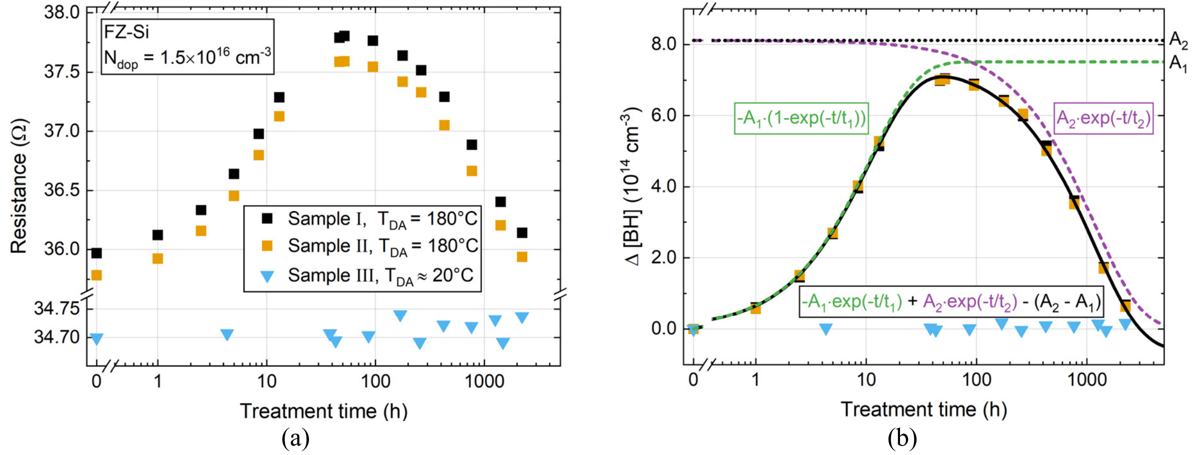

FIGURE 1. (a) Evolution of resistance during a dark anneal at 180°C (samples I+II) or during dark storage at ~20°C. (b) Calculated change in BH pair concentration with respect to the first data point. The black line shows a double exponential fit, the dashed lines the individual components.

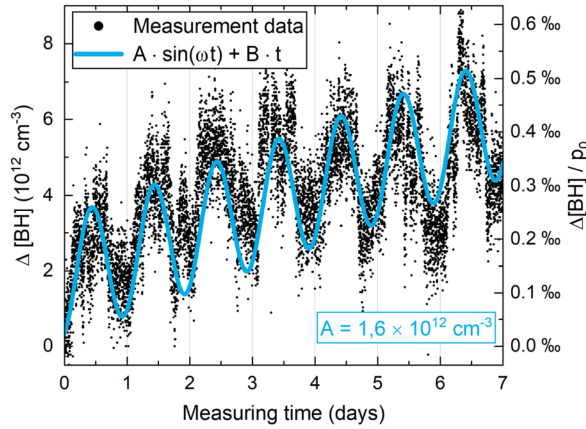

FIGURE 2. Apparent change in BH pair concentration while the sample ($p_0 \sim 1.5\times10^{16}$ cm^{-3}) was left in darkness in the measurement setup at 25°C.

EXPERIMENT 2: DIFFERENT SILICON MATERIAL

In impurity-lean boron-doped FZ-Si, hydrogen predominantly binds to boron simply due to the absence of other binding partners. However, hydrogen is known to bind to many impurities and crystal defects. Thus it is not obvious to what extent BH-dynamics takes place in silicon materials richer in impurities and crystal defects such as Cz-Si or mc-Si. In a second experiment, these materials were exposed to dark annealing at 220°C while changes in hole concentration were monitored. The result is shown in Fig. 3. As can be seen, all materials show a noticeable change in hole concentration Δp_0 that occurs simultaneously pointing to the formation of BH pairs in all samples. However, a direct comparability of the extent is questionable due to differences in doping concentration and peak firing temperature. Especially the released amount of hydrogen from the SiN_x:H layer might differ significantly. In comparison with FZ-Si, hole concentration recovers faster in mc-Si, but it is unclear whether this is due to a faster dissociation of BH pairs, or due to a non-BH-related doping-active effect. In contrast, hole concentration does not recover in Cz-Si, but shows a second increase at around 100 h which strongly accelerates when treatment temperature is raised to 300°C (not shown). It is unclear whether this is due to a non-BH-related doping-active effect. It might be linked to oxygen-related thermal donor (TD) formation which is typically reported to occur at higher temperatures. However, the observed increase might be only the beginning of a by far slower process and it is reported as well that hydrogen seems to catalyse thermal donor formation.

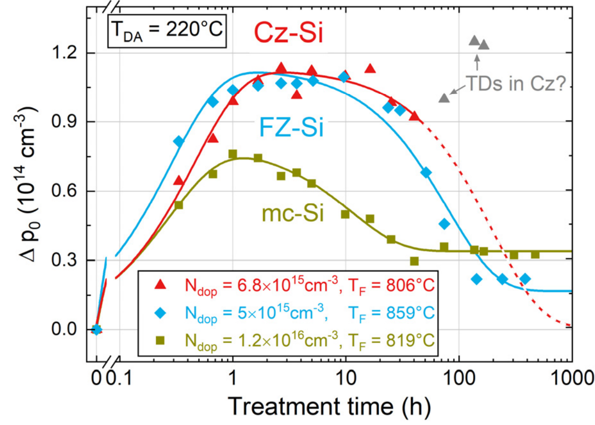

FIGURE 3. Change in hole concentration during dark annealing at 220°C for a FZ-Si, a Cz-Si and a mc-Si sample. The lines represent double exponential fits. For Cz-Si the last gray points are excluded as they might not be related to BH pair dynamics.

EXPERIMENT 3: CORRELATION OF BH AND LeTID DYNAMICS

In the third experiment, boron-doped FZ-Si passivated by AlO_y/SiN_x:H was fired and then dark annealed at 220°C in order to trigger both, BH pair and LeTID dynamics. BH formation was monitored by resistance measurements and effective charge carrier lifetime τ_{eff} was monitored by PCD. Lifetime-equivalent defect densities ΔN_{leq} [25] were derived according to

$$\Delta N_{leq}(t) = \frac{1}{\tau_{eff}(t)} - \frac{1}{\tau_{eff}(t=0)} \tag{10}$$

at an injection $\Delta n = 3\times10^{14}$ cm^{-3} which is close to the cross-over point of FeB and Fe_i [26] [27] rejecting in large parts the unwanted impact of FeB pairing/splitting on ΔN_{leq}. It should be noted that ΔN_{leq} evaluated at a fixed injection level captures both, changes in bulk and surface recombination. Surface recombination is quantified in terms of J_{0s} in the injection range 5-10×10^{15} cm^{-3} relying on a constant-J_0-model [28]. One should note that the J_0 formalism is only valid for sufficiently charged dielectric layers [29] and J_{0s} might be impacted to a certain extent by bulk recombination due to an unfavourable combination of high doping level and low bulk lifetime/high bulk defect densities.

The measured evolution of $\Delta[BH]$, ΔN_{leq} and J_{0s} is depicted in Fig. 4. As can be seen, ΔN_{leq} features two maxima. During the first one (<1 h), J_{0s} remains unchanged indicating that defect formation occurs in the bulk and is likely related to LeTID and its recovery (green background). The second increase of ΔN_{leq} coincides with an increase in J_{0s} indicating that the second maximum is related to a degradation and regeneration of surface passivation (yellow background). For longer times than ~10 h the J_{0s} evaluation algorithm fails probably suggesting that the underlying assumption of a high fixed charge density is violated due to a loss of fixed charges during dark annealing.

In contrast, BH dynamics only exhibits a single, broad maximum (as in the previous experiments). While the initial increase of $\Delta[BH]$ and ΔN_{leq} coincides, the recovery from LeTID sets in by far earlier than the dissociation of BH pairs. In addition, the increase of ΔN_{leq} (logarithmic scale) is more pronounced than that of $\Delta[BH]$ (linear scale). Hence, it can be concluded that BH pairs are most probably not the defect species related to LeTID. Nevertheless, the concurrent formation of BH pairs and LeTID-related defects might indicate a common mode of action. It could be that the dissociation of hydrogen dimers provides atomic hydrogen for subsequent attachment reactions with other impurities like boron or maybe the LeTID-related defect. However, one should note that the expected LeTID-related defect density (in analogy to other known defect species) is of the order of 10^{11} cm^{-3} which is by far smaller than the observed BH pair concentration (10^{14} cm^{-3}) and even below the detection limit level imposed by temperature fluctuations (see Fig. 2). Hence, the presented data do not allow a statement on whether the activation of the LeTID-related defect is due to an attachment of hydrogen (acting as a sink as suggested in [1]), or due to a release of hydrogen (acting as a source as suggested in [30]). Most likely, the observed LeTID and BH dynamics reflect different aspects of hydrogen reactions in crystalline silicon.

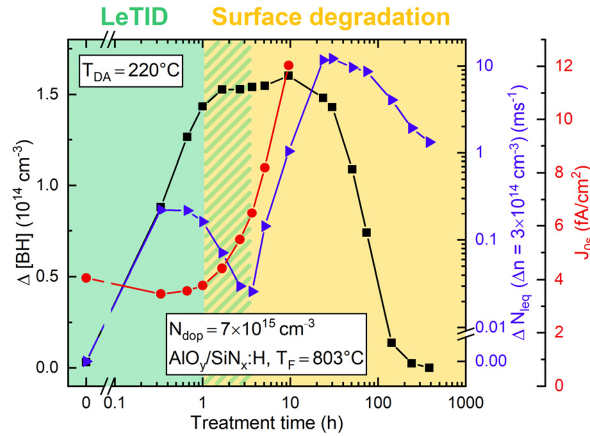

FIGURE 4. Evolution of BH pair concentration $\Delta[BH]$, lifetime-equivalent defect density ΔN_{leq} and surface recombination (quantified by J_{0s}) during dark annealing at 220°C. Lines serve as a guide to the eye.

CONCLUSIONS

The methodology to quantify boron-hydrogen pairs via changes in equilibrium hole concentration in crystalline silicon by means of directly contacted resistance measurements was successfully developed and implemented. Unnoticed temperature fluctuations are found to be the limiting factor for accuracy, suggesting that proper temperature management is the key to highly sensitive measurements. As demonstrated, the used setup can quantify changes in BH pair concentration down to the sub-permille level which corresponds to the low 10^{12} cm^{-3} range for 1 Ω·cm material commonly used for solar cells. The method was used to demonstrate that BH dynamics can be observed not only in impurity-lean FZ-Si, but also in Cz-Si and mc-Si both being richer in impurities and crystal defects. However, other doping-active effects may occur as well. The used sample design also enables lifetime measurements and thus allows for direct comparison of lifetime and BH dynamics on one and the same sample. A comparison with LeTID suggests that BH pairs are probably not the LeTID-related defect species. However, the coincident initial increase in BH pair concentration and LeTID-related defect density may be interpreted as a common mode of action like the splitting of hydrogen dimers.

ACKNOWLEDGMENTS

The authors want to thank Barbara Rettenmaier and Christian Fischer for technical support. Part of this work was supported by the German Federal Ministry of Economic Affairs and Energy under contract numbers 03EE0152A. The content is the responsibility of the authors.

REFERENCES

1. T. H. Fung, M. Kim, D. Chen, C. E. Chan, B. J. Hallam, R. Chen, D. N. Payne, A. Ciesla, S. R. Wenham and M. D. Abbott, Sol. Energy Mater. Sol. Cells **184**, 48-56 (2018).
2. J. Schmidt, D. Bredemeier and D. C. Walter, IEEE J. Photovolt. **9**, 1497-1503 (2019).
3. F. A. Stevie, C. Zhou, M. Hopstaken, M. Saccomanno, Z. Zhang and A. Turansky, J. Vac. Sci. Technol. B **34**, 03H103 (2016).
4. J. I. Pankove, R. O. Wance and J. E. Berkeyheiser, Appl. Phys. Lett. **45**, 1100-1102 (1984).
5. S. A. McQuaid, M. J. Binns, R. C. Newman, E. C. Lightowlers and J. B. Clegg, Appl. Phys. Lett. **62**, 1612-1614 (1993).
6. R. E. Pritchard, J. H. Tucker, R. C. Newman and E. C. Lightowlers, Semicond. Sci. Technol. **14**, 77-80 (1999).
7. C. H. Saeger and R. A. Anderson, Appl. Phys. Lett. **53**, 1181-1183 (1988).
8. T. Zundel, A. Mesli, J. C. Muller and P. Siffert, Appl. Phys. A **48**, 31-40 (1989).
9. R. Rizk, P. de Mierry, D. Ballutaud, M. Aucouturier and D. Mathiot, Phys. Rev. B **44**, 6141-6151 (1991).
10. E. M. Filangeri and T. Nishida, J. Appl. Phys. **76**, 332-335 (1994).

11. M. W. Horn, J. M. Heddleson and S. J. Fonash, Appl. Phys. Lett. **51**, 490-492 (1987).
12. D. C. Walter, D. Bredemeier, R. Falster, V. V. Voronkov and J. Schmidt, Sol. Energy Mater. Sol. Cells **200**, 109970 (2019).
13. A. Herguth and C. Winter, "Methodology and error analysis of direct resistance measurements used for the quantification of boron-hydrogen pairs in crystalline silicon," IEEE J. Photovolt., accepted (DOI: 10.1109/JPHOTOV.2021.3074463) *to be updated in the final version*
14. C. Herring, N. Johnson and C. G. van de Walle, Phys. Rev. B **64**, 125209 (2001).
15. V. V. Voronkov and R. Falster, Phys. Status Solidi B **254**, 1600779 (2017).
16. Mobility Calculator, pvlighthouse.com.
17. D. Klaassen, Solid State Electron. **35**, 953-959 (1992).
18. D. Klaassen, Solid State Electron. **35**, 961-967 (1992).
19. P. P. Altermatt, A. Schenk, B. Schmithüsen and G. Heiser, J. Appl. Phys. **100**, 113715 (2006).
20. R. Pässler, Phys. Rev. B **66**, 085201 (2002).
21. A. Schenk, J. Appl. Phys. **84**, 3684-3695 (1998).
22. R. A. Sinton and A. Cuevas, Appl. Phys. Lett. **69**, 2510-2512 (1996).
23. D. Kiliani, G. Micard, B. Steuer, B. Raabe, A. Herguth and G. Hahn, J. Appl. Phys. **110**, 054508 (2011).
24. E. Schneiderlöchner, R. Preu, R. Lüdemann and S. W. Glunz, Prog. Photovolt. **10**, 29-34 (2002).
25. A. Herguth, IEEE J. Photovolt. **9**, 1182-1194 (2019).
26. G. Zoth and W. Bergholz, J. Appl. Phys. **67**, 6764-6771 (1990).
27. D. H. Macdonald, L. J. Geerligs and A. Azzizi, J. Appl. Phys. **95**, 1021-1028 (2004).
28. A. Kimmerle, J. Greulich and A. Wolf, Sol. Energy Mater. Sol. Cells **142**, 116-122 (2015).
29. K. R. McIntosh and L. E. Black, J. Appl. Phys. **116**, 014503 (2014).
30. W. Kwapil, J. Schön, T. Niewelt and M. C. Schubert, IEEE J. Photovolt. **10**, 1591-1603 (2020).